

DEVELOPMENT OF MAGNETIC BEARING MOMENTUM WHEEL FOR ULTRA-PRECISION SPACECRAFT ATTITUDE CONTROL

Yasushi Horiuchi, Masao Inoue

Mitsubishi Electric Corp., Amagasaki, Hyogo, Japan,
horiuchi@mec.crl.melco.co.jp, inouema@mec.crl.melco.co.jp

Norio Sato

Mitsubishi Precision Co., Ltd., Kamakura, Kanagawa, Japan, sato_norio@mpcnet.co.jp

Tatsuaki Hashimoto, Keiken Ninomiya

Institute of Space and Astronautical Science, Sagamihara, Kanagawa, Japan,
hasimoto@nsl.isas.ac.jp, ninomiya@nsl.isas.ac.jp

ABSTRACT

This paper describes a magnetic bearing momentum wheel (MBMW) for ultra-precise stabilization of spacecraft attitude. For suppressing bearing reaction torque, which disturbs the spacecraft attitude stability, the control bandwidth of the magnetic bearings is designed to be as narrow as possible. Using a prototype of the MBMW, sufficiently quiet and stable rotation up to 8,000 r/min. (64 Nms) is accomplished. Moreover, the accurate measurement of the bearing reaction force and torque showed that small reaction torque remains even if the MBMW rotates in the super-critical speed range. Considering not only the wobbles of the sensor measurement surface but also those of the rotor surface of the bearing, the cause of this residual reaction torque is clarified.

INTRODUCTION

Most of spacecraft are equipped with momentum or reaction wheels for their attitude control. However, the compliance of conventional ball bearing wheel is too small to absorb the large centrifugal force caused by imbalance of the wheel rotor. Accordingly, the ball bearing wheel can be one of the most harmful disturbance sources for the spacecraft attitude stability. Therefore, the focal issue is how to suppress this disturbance. There are mainly two solutions for the disturbance suppression: the first is applying magnetic bearings to the wheel, and the second is installing vibration isolation table between wheel and spacecraft main body. The second solution needs large additional space and weight for the table. Hence, we have applied the magnetic bearing to the momentum wheel.

It is said that there are several possible disturbance sources in magnetic bearings as well as ball bearings. A document [2] pointed out that the disturbance caused by

rotor imbalance, mechanical imperfection of rotor, and so on. Moreover, the Active Vibration Suppression (AVS) methods were discussed for disturbance suppression. This AVS needed so complex procedure that a digital controller was desirable. However, in space environment strong radiation may affect the reliability of the digital AVS circuits.

Considering the radiation, full analog controller is designed for the MBMW in this paper. Using a prototype of the MBMW and a Disturbance Measuring Device (DMD) with a vacuum vessel, wheel rotation evaluations and disturbance measurements were implemented. Moreover, this paper describes the MBMW's mechanical design, controller design and disturbance measurement results. The modeling of the disturbance is also discussed.

MECHANICAL DESIGN

Besides the disturbance coming from the MBMW, other internal and external torque disturb the attitude stability of the spacecraft. Accordingly, there is an acceptable disturbance level for the MBMW as shown in **FIGURE 1**. This disturbance level is based on the

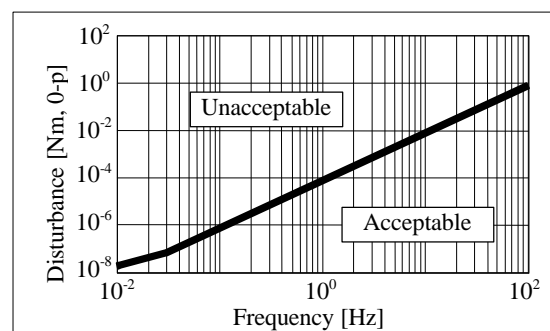


FIGURE 1: Acceptable disturbance level

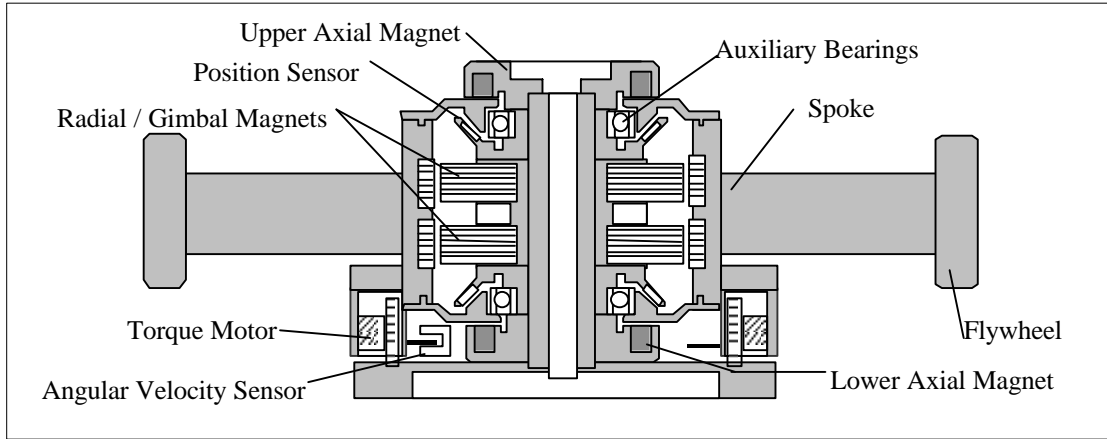


FIGURE 2: Cross section of MBMW

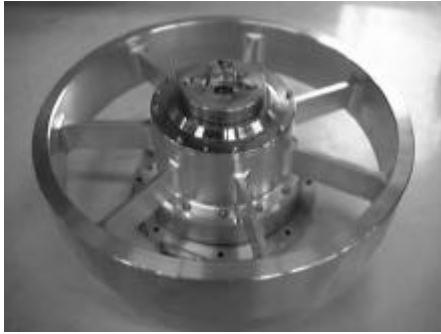


FIGURE 3: Perspective view of MBMW



FIGURE 4: Stator of MBMW

requirement for SOLAR-B [1], which will be launched in the year of 2004.

We determined the specification of the MBMW, such as a rotor size and a rotation speed range, based on the AOCS requirement of the spacecraft. **FIGURE 2-4** illustrate a cross section, a perspective view, and stator of the MBMW, respectively. **TABLE 1** shows major specifications of the MBMW, and the parameters of the magnetic bearings are summarized in **TABLE 2** in detail. For reducing iron loss, the rotor elements of the radial magnetic bearings consist of soft magnetic iron sheets. Because the control currents in the windings are almost constant when the rotation speed is high, the magnetic fields in the stator elements are also almost

TABLE 1: Fundamental specification of MBMW

| Item | Note |
|-------------------|--|
| Bearing | 5-axis active magnetic bearings |
| Angular momentum | 30 Nms @ 5,000 r/min. |
| Rotation speed | Max. 8,000 r/min. |
| Mass | Total 9.0 kg, rotor 5.1 kg |
| Moment of inertia | 0.0573 kgm ² (around spin axis) |
| Size | φ 350 mm, 150 mm (height) |
| Gimbaling angle | +/- 0.1 deg. |
| Motor torque | Max. 0.05 Nm |
| Power consumption | 15 W (steady) |

TABLE 2: Parameters of magnetic bearings

| | Item & value | |
|------------------------------|---|-------|
| | Radial magnets NNSS configuration | Poles |
| Pole area [mm ²] | | 144 |
| Number of winding turns | | 300 |
| Nominal gap [mm] | | 0.8 |
| Axial magnets | Poles | 2 |
| | Pole area [mm ²] | 800 |
| | Number of winding turns | 300 |
| | Nominal gap [mm] | 0.5 |
| Sensors | Eddy current type | 8 |

constant. Accordingly, the stator elements are made of solid (not laminated) iron.

In order to measure the disturbance force and torque due to the MBMW, we have developed a Disturbance Measuring Device (DMD) with a vacuum vessel as



FIGURE 5: Disturbance Measuring Device

shown in **FIGURE 5**. This DMD consists of following major components:

- Vacuum vessel for wind loss reduction,
- 6 load cells in Steward Platform for 6-axis force and torque detection,
- Air suspension table for isolating external force,
- Electronic circuit and personal computer for disturbance calculation and FFT analysis.

The detecting resolution of the DMD is 8.7×10^{-4} [N] for each load cell output. This limit is due to a quantization error at A/D conversion.

There are two frames of reference on the wheel rotor. The first frame of reference (F_1) coincides with the principal moment of inertia axes of the rotor, and the second one (F_2) is based on the location of the sensors and the electromagnets. However, F_1 differs from F_2 because the motor, which is attached on the lower end of wheel spin axis, shifts the center of mass of wheel rotor. Accordingly, the force on the F_2 behaves as a translational force and as a rotational torque on the F_1 . Similarly, the gimbaling angle of the wheel on the F_1 is detected as a gimbal motion and a translational motion on the F_2 . Thus, the translation and the gimbaling of the MBMW interfere each other at the displacement detection and the magnetic control force generation. Because this geometric interference makes the disturbance worse, a method of canceling out such interference is described in the following section.

In order to reducing this geometric interference, we will redesign the wheel configuration including the motor position for the engineering model of the MBMW.

CONTROLLER DESIGN

The controller for the magnetic bearings of the MBMW consists of 6 stages except of the sensors and electromagnets:

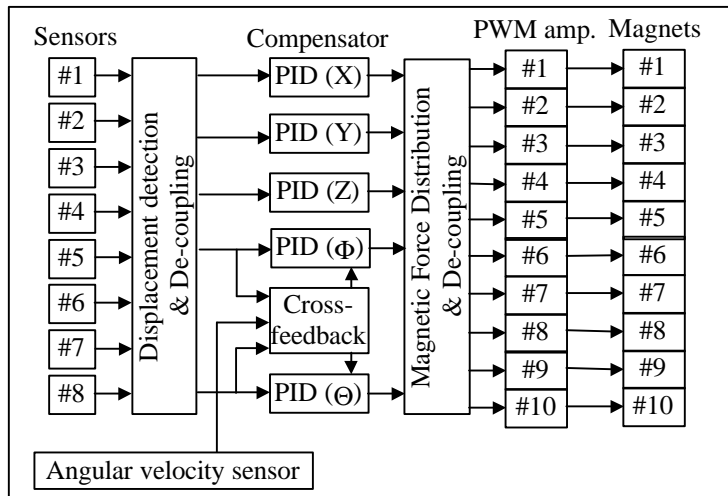


FIGURE 6: Magnetic bearing controller

- Displacement detection stage;
8 sensors output 5 axes displacements (X, Y, Z, Φ , and Θ), and Low-Pass Filtered (300 – 600 Hz cutoff).
- Sensor signal de-coupling stage;
Canceling out the geometric interference in the displacement detection.
- Compensation stage;
Full analog conventional PID controller for main and PD cross-feedback controller between two gimbal axes for precession and nutation damping.
- Force signal de-coupling stage;
Canceling out the geometric interference in the force / torque generation.
- Notch filter stage;
Eliminating the force / torque at the frequency of the wheel rotation.
- Power amplifier stage;
Winding current controller with PWM by modulation frequency 20 kHz for radial magnets, and 5 kHz for axial magnets.

The total magnetic bearing controller is illustrated in **FIGURE 6**. If the variation of the air gap at the electromagnet is negligibly small compared with the nominal gap, the actual magnetic force is nearly proportional to the square of the winding current. For linearization of the characteristic of the electromagnets, there is an analog multiplier in the feedback loop of the power amplifier (**FIGURE 7**). Thus, the square of the current, which is proportional to the actual electromagnetic force, is fed back to the current controller.

We designed the MBMW controller parameters in order that the control bandwidth became as follows:

| | |
|--------|-------|
| Radial | 15 Hz |
| Gimbal | 10 Hz |
| Axial | 40 Hz |

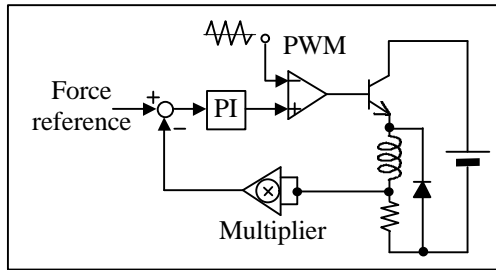


FIGURE 7: Current control loop

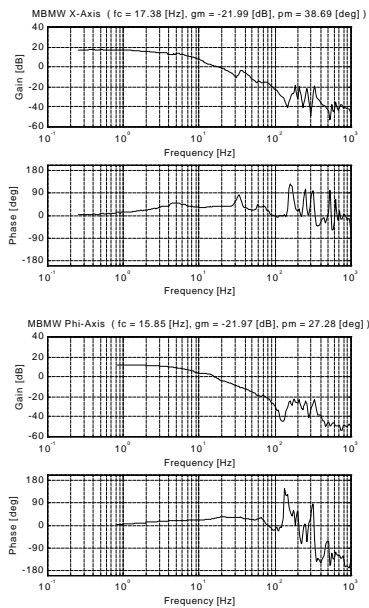


FIGURE 8: Open-loop transfer function of MBMW (upper: radial, lower: gimbal)

Axial control bandwidth is higher than other axes because axial controller must support the gravity of the wheel rotor. Hence, it can be no more than 15 Hz in an actual micro-gravity environment.

FIGURE 8 illustrates the measured open-loop transfer functions of the MBMW. The crossover frequencies of a radial and a gimbal axis are 17 Hz and 16 Hz, respectively. The cross-feedback controller for gimbal axes is enabled when the wheel rotation is over 2,000 r/min.

DISTURBANCE MEASUREMENT

The magnetic bearing controller evaluations indicate that the designed MBMW brings satisfactorily stable and quiet wheel suspension up to 8,000 r/min. Using the DMD, the rotor balancing and the disturbance force/torque measurement under various test conditions are implemented.

FIGURES 9 and **10** show examples of the measured disturbance in low-to-mid frequency range (mainly 0.1 – 10 Hz) and that in high frequency range (above 10

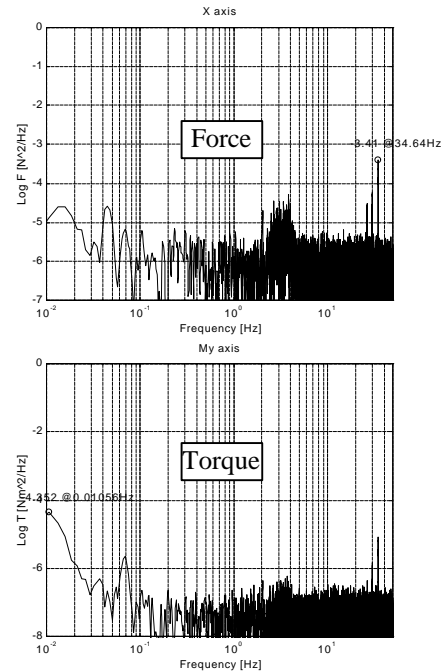


FIGURE 9: Disturbance at 6,000 r/min.

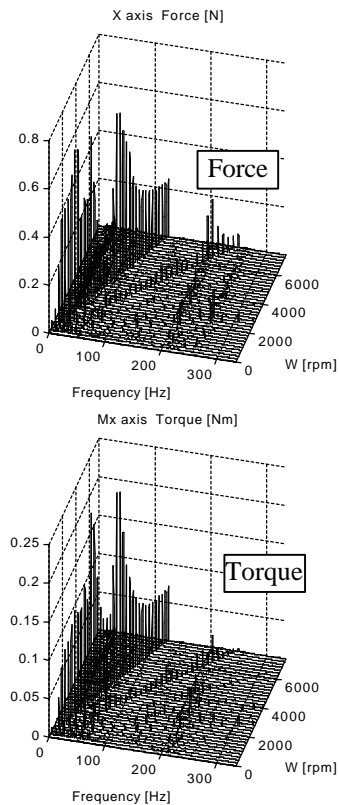


FIGURE 10: Disturbance in high frequency range

Hz), respectively. The disturbance in low-to-mid frequency range has no distinct frequency component, so that it is given in the form of Power Spectral Density (see **FIGURE 9**). Considering the effect of the air suspension table's natural frequency at 3-4 Hz, one can

obtain the magnitude of the disturbance as shown in **TABLE 3**.

TABLE 3: Disturbance (0.1-10 Hz)

| Disturbance | Magnitude in PSD |
|-------------|--|
| Force | $< 1 \times 10^{-5}$ [N ² /Hz] |
| Torque | $< 1 \times 10^{-6.5}$ [(Nm) ² /Hz] |

In the high frequency, the distinct frequency component coincides with wheel rotation speed, and the disturbances have two peaks at about 15 Hz and 80 Hz (see **FIGURE 10**). The former frequency coincides with the natural frequency of the AMB, and the latter corresponds to that of DMD structure. Therefore, these two peaks are reasonable.

Note that, in high-speed rotation, the magnitude of disturbance gets closer to a certain non-zero value, which is irrelevant to the wheel rotation speed. At the same time, the detected X-Y and Φ - Θ motions of rotor show almost circles, whose radii are about 13 μm and 9×10^{-3} [deg], respectively. These results mean that:

- Wheel rotates roughly around its principal axis of inertia in its high-speed rotation,
- Static and dynamic imbalances are about 13 μm and 9×10^{-3} [deg], respectively.

Since further precise static and dynamic balancing of the rotor will be implemented for the engineering model of the MBMW, we can reduce these imbalances.

Modeling of Disturbance Sources

It is said that the most possible disturbance source is the sensor noise, such as wobbles of sensor measurement surface [2]. In addition, the wobbles of magnetically attracted rotor surface at radial bearings may cause the disturbance. This process is as follows.

- Assume that, in high-speed rotation, sensor noise is successfully rejected by notch filter for example,
- Steady force commands make bearing currents to be constant (nearly equal to bias currents),
- While air gaps at the bearings vary in sync with wheel rotation as well as sensor noise,
- Actual magnetic force and torque vary in accord with wheel rotation.

Therefore, even if notch filters eliminate the sensor noise sufficiently, the gap wobbles at the magnetic bearings actually cause the disturbance.

The magnitude of the disturbance caused by the sensor noise, D_s , and that caused by the gap wobbles, D_G , are described by Eqs. (1) and (2), respectively.

$$D_s = K_s \delta g_s \quad (1)$$

$$D_G = K_G \delta g_G \quad (2)$$

where

K_s : Equivalent active bearing stiffness = $m \omega^2$,
 K_G : Equivalent passive bearing stiffness

$$= -\frac{n\mu_0(NI)^2 S}{2g_0^3},$$

δg_s : Sensor noise including wobbles,
 δg_G : Air gap variation at radial magnet,
 m : Rotor mass = 5 [kg]
 ω : Crossover frequency = 15 [Hz]
 n : Equivalent number of magnets = 4
 μ_0 : Magnetic permeability in vacuum
 NI : Nominal magnetomotive force = 100 [A]
 S : Area of magnetic pole = 144 [mm²]
 g_0 : Nominal air gap at radial magnets = 0.8 [mm]

Substituting $\delta g_s = \delta g_G = 13$ [μm] and these parameters, one can obtain

$$D_s = 0.57 \text{ [N]}, \quad D_G = 0.10 \text{ [N]}.$$

Because the actual disturbance in radial translation is 0.2 [N] (see **FIGURE 10**), it is still unknown which disturbance source is dominant.

Consideration of Disturbance Source

In order to identify the disturbance source, we examined whether notch filters and nominal air gap expansion were effective. The notch filters were inserted into the force/torque commands of all 5 axes of the magnetic bearing controllers. The nominal air gap at radial/gimbal magnets was expanded by exchange of the rotor elements of the magnetic bearings.

TABLE 4 shows the disturbance comparison at 6,000 [r/min.] under these conditions. The large air gap provided slight disturbance decrease, while the notch filters have sufficiently reduced the disturbances. Moreover, linearization of the power amplifiers brought further suppression to the harmonic of the disturbance.

TABLE 4: Disturbance comparison at 6,000 r/min.

| Conditions | Disturbances |
|---------------|--------------------------|
| | Radial [N] / Gimbal [Nm] |
| (1) A-, B-, C | 0.32 / 0.068 @ 100 Hz |
| | 0.11 / 0.020 @ 200 Hz |
| (2) A-, B-, D | 0.22 / 0.058 @ 100 Hz |
| | 0.10 / 0.021 @ 200 Hz |
| (3) A+, B-, D | 0.078 / 0.015 @ 100 Hz |
| | 0.18 / 0.029 @ 200 Hz |
| (4) A+, B+, D | 0.093 / 0.017 @ 100 Hz |
| | 0.081 / 0.011 @ 200 Hz |

A-: without notch filter

A+: with notch filter

B-: without multiplier in current feedback loop

B+: with multiplier in current feedback loop

C: nominal air gap 0.4 mm at magnetic bearings

D: nominal air gap 0.8 mm at magnetic bearings

Under the conditions of (3) or (4), the measured disturbance force is practically same as the calculated disturbance D_G . Accordingly, if the disturbance D_S is negligibly small thanks to the notch filters, it will be reasonable to regard D_G as the distinct component of the residual disturbance.

Note that the disturbance caused by sensor noise, D_S , is suppressible by using the notch filters, but that the disturbance due to the air gap variation at magnets, D_G , can not be reduced. D_G essentially depends upon the processing and/or assembly accuracy of the rotor parts. Hence, any Active Vibration Suppression (AVS) [2] is useless for further disturbance suppression, if there is no improvement on the static and dynamic balancing of the wheel rotor.

In this consideration, we used analog-type notch filters, which had 100-Hz fixed notch frequency. Therefore, the wheel rotation speed was available only at 6,000 [r/min.]. When more advanced notch filters are installed, such as tracking notch filters, satisfactory disturbance suppression will be obtained in the wide wheel speed range. Moreover, the engineering model of the MBMW, whose rotor is well balanced, will bring further disturbance suppression.

SUMMARY

The authors have newly developed a prototype of Magnetic Bearing Momentum Wheel (MBMW) for an ultra-precise spacecraft attitude stabilization. Using a Disturbance Measuring Device (DMD), the disturbance force and torque caused by the MBMW have been measured.

Firstly, the rotor was balanced from the point of view of minimizing the disturbances. Secondly, the disturbance measurements under several different conditions were implemented. Thirdly, the theoretical disturbance force was analyzed. Finally, based on this comparison and the analysis, the residual disturbance was identified. Its distinct component was the disturbance due to the air gap variation at magnets. This disturbance essentially depends upon the processing and/or assembly accuracy of the rotor parts. Therefore, any control device is useless for further disturbance suppression.

In addition, the finally obtained disturbance level barely satisfies the specification required for ultra-stable attitude control of spacecraft SOLAR-B.

REFERENCES

- [1] T. Shimizu and The Solar-B Working Group, "Solar-B -- The Next Japanese Solar Mission --", Solar Physics with Radio Observations, Proc. of the Nobeyama Symposium (NRO Report No. 479 edited by T. Bastian, N. Gopalswamy, and K. Shibasaki), 1999.
- [2] U. J. Bichler, "A Low Noise Magnetic Bearing Wheel for Space Application", Proc. of the 2nd International Symposium on Magnetic Bearings, Tokyo, 1990.